Front. Earth Sci. 2016, 10(2): 274–291
DOI 10.1007/s11707-016-0558-3

RESEARCH ARTICLE

Effectiveness of basin morphometry, remote sensing, and applied geosciences on groundwater recharge potential mapping: a comparative study within a small watershed

Suvendu ROY (✉), Abhay Sankar SAHU

Department of Geography, University of Kalyani, Kalyani, Nadia-741235, West Bengal, India

Abstract A multidisciplinary approach using the integrated field of geosciences (e.g., geomorphology, geotectonics, geophysics, and hydrology) is established to conduct groundwater recharge potential mapping of the Kunur River Basin, India. The relative mean error (RME) calculation of the results of three applied techniques and water table data from twenty-four observation wells in the basin over the 2000 – 2010 period are presented. Nine sub-basins were identified and ranked for the RME calculation, where the observation wells-based ranking was taken as standard order for comparison. A linear model has been developed using six factors (drainage density, surface slope, ruggedness index, lineament density, Bouguer gravity anomaly, and potential maximum water retention capacity) and a grid-wise weighted index. In a separate comparative approach, the sub-basin and grid-wise analyses have been conducted to identify the suitable spatial unit for watershed level hydrological modeling.

Keywords groundwater, basin morphometry, SCS curve number, geosciences, geoinformatics

1 Introduction

Groundwater being an important resource, an understanding of the hydro-geological processes and identification of the potential areas for its withdrawal and recharge is important (Samadder et al., 2011). Long-term over-exploitation of groundwater has created many challenges to effective water management in India (Shankar et al., 2011). As compared to the rest of the world, a large quantity of groundwater is continuously used for agricultural purposes in India, reaching about 61% during 2000–2001 to 2006–2007 (Shah, 2009, 2011). Irrigation using groundwater resources has increased at a very rapid rate since the 1970s as is evident from the growing number of groundwater irrigation facilities (wells, tube wells, etc.) in the country (Minor Irrigation Census, 2001). According to Kumar and Raj (2013), the per capita availability of water in India has declined from 3,000 m^3/year to 1,800 m^3/year from 1951 to 2010. The share of surface water has also declined from 60% in the year of 1950 to 30% on the first decade of the 21st century respectively (CGWB, 2010).

However, suitable methods for mapping potential groundwater recharge areas is still problematic. The purpose of the current investigation is to determine, test, and demonstrate the methods for a successful and efficient mapping of the groundwater recharge potential over a small drainage basin. The present study deals with basin morphometry based on topographical sheets (1: 50,000), remote sensing techniques, SCS Curve Number method, and the integrated field of geosciences to consider suitable method towards mapping the Kunur River Basin (KRB). The study has also evaluated the effectiveness of sub-basin scale and grid based mapping in groundwater research.

2 Basin morphometry and groundwater

Basin morphometry is one of the key elements to study the surface and sub-surface hydrological conditions in any drainage basin (Obi Reddy et al., 2004; Subba Rao, 2009; Martins and Gadiga, 2015). Prioritization techniques have been widely used to prepare the sub-basin scale groundwater potentiality map in India (Krishnamurthy et al., 1996; Biswas et al., 1999; Khan et al., 2001; Suresh et al., 2004; Nooka Ratnam et al., 2005; Thakkar and Dhiman, 2007; Srinivasa et al., 2008; Javed et al., 2009; Avinash et al., 2011; Banerjee et al., 2011; Avinash et al., 2014) and throughout the world (Esper Angillieri, 2008; Elmahdy

Received September 10, 2014; accepted September 18, 2015

E-mail: suvenduroy7@gmail.com

and Mohamed, 2015). Quantitative assessment of basin morphometric parameters (linear, areal, and relief) help reveal information about lithology, hydrological regime, and operating exogenic/endogenic processes within the basin, which are very useful to correlate with groundwater development (Avinash et al., 2011; Magesh et al., 2013; Saravanan and Manjula, 2015; Zhang et al., 2015).

According to Strahler (1964), a lower number of streams in a sub-basin indicates the maturity of that topography and a higher number of streams (first and second orders) indicates the sub-basin is prone to erosion. A bifurcation ratio (R_b) within the range of three to five indicates no influence of geological structure over the basin (Strahler, 1964). According to Pakhmode et al. (2003), a watershed having a lower R_b value indicates uniform underlying material and systematic stream networking. Permeability of the underlying rock controls the length and number of streams within the basin; a lower number of relatively longer streams are observed over permeable rock strata and vice-versa (Pakhmode et al., 2003; Rajwant and Sharma, 2015; Saravanan and Manjula, 2015).

The shape of a basin plays an important role in defining the hydrologic condition of a watershed (Horton, 1932; Hajam et al., 2013). A high value of the elongation ratio (E_R) indicates active denudational processes associated with high infiltration capacity and low surface runoff over the basin, whereas a low E_R value indicates a higher elevation of the basin and increased susceptibility to high head-ward and tectonic lineament erosion (Obi Reddy et al., 2004; Manu and Anirudhan, 2008; Rajwant and Sharma, 2015). According to Schumm (1956), an E_R value close to 1.0 indicates a region of low relief; values ranging from 0.6 to 0.8 are generally associated with regions of high relief and steep ground slopes. Hence, the E_R value of KRB indicates the study area is one of high relief and steep slopes.

The circularity ratio (C_r) is more influenced by stream length, stream frequency (S_f), and the gradients of streams of different orders rather than the slope conditions and drainage pattern of a basin (Strahler, 1964). Low, medium, and high values of C_r define young, mature, and old stages of tributaries in a basin respectively. If the C_r value is 1.0 then the basin will be a perfect circle in shape and discharge quantity will be high (Miller, 1953). The compactness coefficient (C_c) is defined as a ratio between the length of the drainage basin boundary (the perimeter) and the perimeter of a circle having the same area, where the resultant value 1.0 indicates a perfectly circlular basin (Gravelius, 1914; Hidore, 1964; Reddy, 2005).

For drainage density (D_d), Horton (1945) stated that lower values of D_d indicate permeable strata under dense vegetation and low relief, whereas higher values of D_d indicate impermeable rocks under sparse vegetation and the areas with mountainous relief. The high value of stream frequency indicates greater surface runoff and a steep ground surface (Horton, 1932, 1945). The interaction between basin hydrology, vegetation cover, soil texture and structure, and channel spacing statistically are determined by the drainage texture (D_t) (Horton, 1945; Smith, 1950; Schumm, 1956). Smith (1950) had classified D_t as coarse (< 4 per km), intermediate (4–10 per km), fine (10–15 per km) and ultra-fine (> 15 per km). Here, the KRB deals with the coarse texture surface due to the lower value of D_t (< 1.0).

According to Schumm (1956), C_m, the constant of channel maintenance, is the inverse characteristic of drainage density (D_d), which depends on rock type, permeability, climatic regime, vegetation cover, and relief, and also the duration of erosion. The length of overland flow (L_o) is used to describe the length of surface water flow before its merging in the nearest stream channels (Horton, 1945). According to Horton (1945), L_o plays a crucial role in controlling the hydrological and physiographical developments of drainage basins. Several other relief aspects, e.g., basin relief (B_r), relief ratio (R_r), ruggedness index (RI), basin average slope (S), and stream gradient (S_g), also control the hydrological characteristics of any basin (Schumm, 1956; Strahler, 1957; Hadley and Schumm, 1961; Sreedevi et al., 2005; Avinash et al., 2014; Saravanan and Manjula, 2015).

3 Remote sensing and groundwater

The operational uses of satellite data in water resource monitoring were developed in the early 1980s (Ramamoorthi, 1983). Since then , the optical remote sensing and radar imageries have not been able to penetrate beyond the uppermost surface layer (~1 m) (Schultz, 1997; Wagner et al., 2007). The Australian Water Resources Assessment (AWRA), the Center for Remote Sensing and Mapping Science (CRMS) at the University of Georgia (UGA), the Indian Space Research Organization (ISRO), the Center for Space Research (CSR) at University of Texas, and the Groupe de Recherche de Géodésie Spatiale (GRGS) are all continuously working to improve the accuracy and spatial detail of hydrological model estimates and to validate the new updated technique in groundwater storage (GWS) change monitoring.

Recently, the Gravity Recovery and Climate Experiment (GRACE), is being used to collect daily and monthly variations of sub-surface water storage by measuring the anomaly in earth's gravity with a combination of land surface models (e.g., multilayer perceptron (MLP)) and artificial neural network (ANN) models (Longuevergne et al., 2010; Long et al., 2013, 2014). Using GRACE data, water science researchers can eliminate questions about the accuracy of traditional monitoring techniques, those that depend on site measurements or model simulations, and are typically costly and time-consuming (Jiang et al., 2014). Wahr et al. (2004) reported that GRACE data are able to detect the changes of total water storage (TWS)

within the accuracy of 1.5 cm on a wide range of spatial scales (minimum footprint > 200,000 km^2) and seasonal time scales.

Since the beginning of twenty-first century, GRACE has been an excellent option for hydrological research, but its limitation is that it is suitable for continental-scale study only (> 200,000 km^2) not at smaller, regional scales. In this study, multispectral optical imageries are used for micro level hydrological modeling in the Kunur River Basin. According to Meijerink (1996), the synergism of satellite imagery and airborne geophysical data can be a valuable asset in the early stages of groundwater exploration and in groundwater modelling. The imaging sensors can sometimes detect subsurface features such as buried channels and dry vadose zones without vegetation (McCauley et al., 1982; Koopmans, 1983; Drury, 1993; Prakash and Mishra, 1993; Roy and Ray, 1993; Chaudhary et al., 1996; Meijerink, 1996; Ravindran and Jeyram, 1997; Godebo, 2005).

During the last two decades, many works have been published on the potential application of remote sensing to hydrological data extraction (Rango and Ritchie, 1996; Guo et al., 2015; Menenti et al., 2015). Thermal bands, multispectral imageries, and synthetic aperture radar (SAR) data have been used to collect information regarding groundwater potential and deficit regions along with the flow systems of groundwater (Meijerink, 1996; Shi et al., 1997; Elbeih, 2015). Ringrose et al. (1998) studied the possible association of near-surface groundwater and vegetation characteristics using a combination of remote sensing data and GIS techniques. De Alwis et al. (2007) studied the application of normalized difference vegetation index (NDVI) and normalized difference water index (NDWI) techniques to delineate saturated surface areas and hydrological active areas (HAA) for water resource planning. Van Dijk and Renzullo (2011) introduced spatial water resource monitoring systems (SWRMS) to provide valuable information on water management with the help of satellite observations.

4 Materials and methods

4.1 Selected area for case study

The Kunur River Basin (KRB) is a small watershed (~916.40 km^2) within the interfluve of the Ajay and Damodar Rivers (Fig. 1). It lies in the northeastern part of the Barddhaman District in West Bengal, India. The Kunur River is a major right bank tributary of the Ajay River. KRB covers almost 33% of the lower Ajay river basin. The river originates in the western upland of the Barddhaman District at an altitude of 125 m. It runs for a distance of 114 km towards the east. The elevation of the catchment basin ranges from 131 m on the sandstone plateau to 20 m at the confluence point with the Ajay River (Roy and Mistri, 2013). The forest cover of this basin is almost 31.35% of the area; water covers around 10.35%, 13.82% is for human settlement, 41.74% for agricultural land, and 2.73% of the area comes under the category of barren land or unsuitable areas for agriculture (based on Landsat 8 Image, dated on 26th April, 2013; processing by Q-GIS v.2.4, at 97.56% of accuracy). From the spatial science perspective, this basin is tropical; the Tropic of Cancer (23° 30′ E) passes through the KRB from West to East.

From 1901 to 2003, the average annual rainfall in the

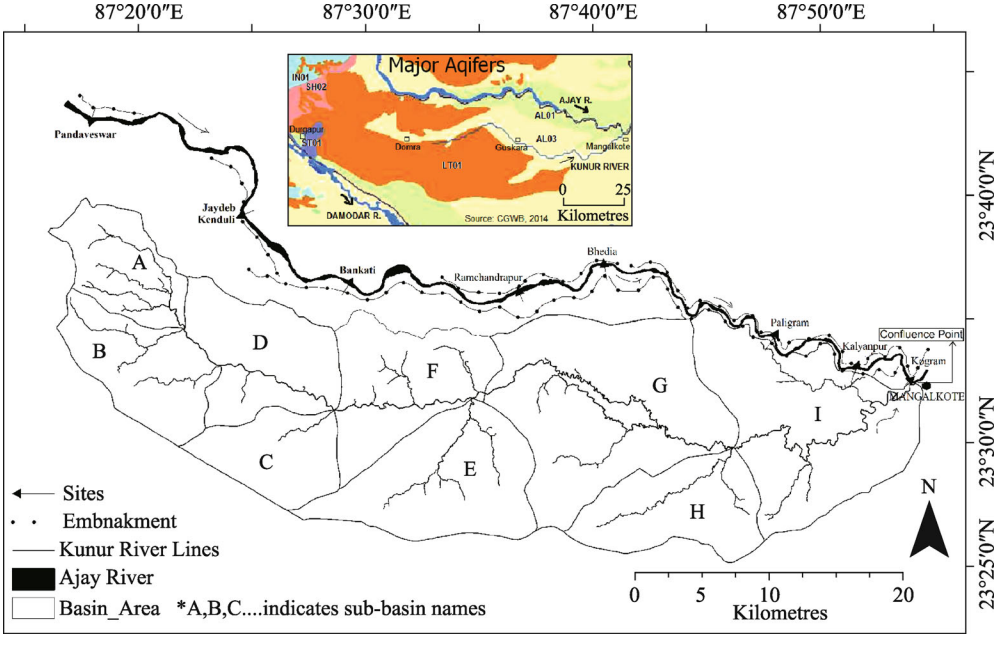

Fig. 1 Location map of the study area with sub-basins and major aquifer system over the Ajay-Damodar interfluve (inset) (Source: CGWB, 2014).

region was 1,380 mm with a mean annual temperature of 25.8°C (IMD, 2014). According to the National Climate Centre (2006) of India Meteorological Department, the total amount of rainfall during the month of September has increased throughout the South Bengal region (56.50 mm at 95% significance level). Seasonal rainfall is increased during the monsoon (91 mm), post-monsoon (26 mm), and annual (95 mm) rainfall respectively, at 90% level of significance for the last 100 years (1901 – 2003).

The study area consists of six major aquifer systems with varying characteristic of bed thickness, groundwater depth, and water yield capacity (Table 1 and Fig. 1-inset) (CGWB, 2014). The laterite aquifer covers 58% of the basin area and extends from the middle to the top of the basin. It has a low yield capacity (20 – 60 m^3/day). The downstream area of the basin is covered by alluvial aquifers (37.88% of the total basin area) with high yield capacities. The upper edge of the basin consistes of sandstone, shale, and fine-grained siltstone with coal seams. An eastward sub-surface flow of groundwater is present with ranging range of electric conductivity from 500 to 2000 micro-Siemens/cm. CGWB (2014) states two major administrative units, Mangalkote and Bhatar, in the downstream area of KRB are in a semi-critical zone because of the groundwater susceptibility (CGWB, 2014).

4.2 Morphometric indices

The boundary of the KRB has been delineated using Survey of India (SoI) topographical maps (73 M/6, M/7, M/10, M/11, M/14, and M/15; scale of 1:50,000, 1967 edition) and Landsat 7 ETM+ images. All topographical maps were geo-referenced into a Universal Transverse Mercator (UTM) projection, WGS 84, Zone 45 North using 16 ground control points (GCPs) distributed at all the corners for each map in < 0.002 root mean square (RMS) error. The entire KRB has been split into nine major sub-basins (A to I) based on the land surface characteristics (more than 60% area under a single category), drainage pattern, and variation of relief. To identify the sub-basin-wise variation of groundwater recharge potential, eighteen morphometric indices have been calculated for all nine sub-basins using geoinformatics technology. Applied techniques for these eighteen indices have been explained in Table 2 with proper references. The role of individual morphometric indices on groundwater development has been explained in the same table with bivariate correlation, where the positive sign indicates groundwater recharge potential is increasing with higher morphometric values of a particular parameter and an inverse condition for the negative sign.

4.3 Applied remote sensing and hydrology: SCS curve number method

The hydrological behaviour of a watershed is primarily controlled by the rate of infiltration and the amount of direct runoff (Wagener et al., 2004; Ajmal et al., 2015). To incorporate the effects of land cover types (Falkenmark, 1994; Ringrose et al., 1998) and hydrological soil groups (Anbazhagan et al., 2005) on the rate of infiltration and rainwater retention, the Soil Conservation Services (SCS) Curve Number (CN) method has been applied to estimate basin-wise potential maximum water retention capacity of the soil during heavy rainfall. The SCS curve number method is a simple, widely used, and efficient method for determining the approximate amount of direct runoff and water loss from a rainfall event over an area of interest, in which the effect of land use and land cover, various soil characteristics, and antecedent moisture conditions are also considered (Chow, 1964; United States Department of Agriculture et al., 1999; Anbazhagan et al., 2005; Shi et al., 2009). According to United States Department of Agriculture et al. (1999), this technique helps to estimate the water retention capacity of soil for a particular region, which is a vital indicator for groundwater development. The SCS curve number method was originally developed by the Soil Conservation Service (1972) for the develop-

Table 1 The major aquifers in the study area and their different characteristic with geological formation period and covering area in the KRB (Source: CGWB, 2014)

Code	Name	Depth of water level (Decadal Average in m bgl)	Thickness of aquifer/weathered zone/m	Yield /($m^3 \cdot day^{-1}$)	Age	% of the total KRB
AL01	Younger alluvium (clay/silt/sand/ calcareous concretions)	5 – 10	50 – 700	200 – 1500	Quarternary	3.81
AL03	Older alluvium (silt/sand/gravel/ lithomargic clay)					34.07
LA01	Laterite/ferruginous concretions	5 – 10	8 – 20	20 – 60		58.00
ST01	Sandstone/ conglomerate	5 – 10	5 – 40	5 – 2000	Upper Palaeozoic	0.28
SH02	Shale with sandstone	5 – 15	10 – 30	20 – 80	to Cenozoic	2.67
IN01	Basic rocks (dolerite, anorthosite etc.)	5 – 15	5 – 25	Low Yield	Proterozoic to Cenozoic	1.17

Table 2 Techniques of different morphometric indices and their relationship with groundwater development

Morphometric parameters	Formulas	Followed by	Role or relation with groundwater development	Applied by
Stream Order (u)	Hierarchical rank	Strahler (1964)	(–ive)	
Stream Frequency (S_f)	$S_f = \Sigma N_u / A$ where S_f = Stream frequency; ΣN_u = Total no. of streams of all orders; A = Area of the Basin (km^2)	Horton (1932, 1945)	(–ive)	Biswas et al., 1999; Subba Rao, 2009
Drainage Density (D_d)	$D_d = \Sigma L_u / A$ where D_d = Drainage Density (km/km^2); ΣL_u = Total length of streams of all orders in km; A = Area of the Basin (km^2)	Horton (1932, 1945)	(–ive)	Todd and Mays, 2005
Drainage Texture (D_t)	$D_t = D_d \times S_f$ where S_f = Stream frequency and D_d = Drainage Density (km/km^2)	Horton (1945)	(–ive)	Smith 1950; Kale and Gupta, 2001
Stream Length Ratio (S_{tr})	$S_{tr} = L_u / L_{u-1}$ where, Lu = Total stream length of order ' u '; L_{u-1} = The total stream length of its next lower order	Horton (1945)	(–ive)	Pakhmode et al., 2003; Sreedevi et al., 2005
Bifurcation Ratio (R_b)	$R_b = Nu / N_{u-1}$; where R_b = Bifurcation ratio; N_u = Total no. of stream segments of order ' u '; N_{u-1} = Number of segments of the next higher order	Schumm (1956)	(–ive)	Pakhmode et al., 2003; Biswas et al., 1999; Avinash et al., 2011
Mean Bifurcation Ratio (BR)	B_R = Average of bifurcation ratios of all orders	Strahler (1957)	(–ive)	
Form Factor (F_f)	$F_f = A / L^2$ where, A = Area of the basin (km^2); L = Basin length (km)	Horton (1932, 1945)	(–ive)	Biswas et al., 1999; Subba Rao, 2009
Elongation Ratio (E_R)	$E_r = 1.128\sqrt{(A / L)}$ where, A = Area of the basin (km^2); L = Basin length (km)	Schumm (1956)	(+ ive)	Obi Reddy et al., 2004, Manu and Anirudhan, 2008
Circularity Ratio (C_r)	$C_r = 4 \pi A / P^2$ where, A = Area of the basin (km^2); P = Perimeter (km); π = 3.1415	Miller (1953), Strahler (1964)	(–ive)	Miller,1953; Biswas et al., 1999; Avinash et al., 2011
Shape Factor (SF)	$Bs = L^2 / A$ where, L = Basin length (km); A = Area of the basin (km^2)	Horton (1932)	(+ ive)	Biswas et al., 1999
Compactness Co-efficient (C_c)	$C_c = 0.2821 P / A^{0.5}$ where, P = Perimeter (km); A = Area of the basin (km^2)	Gravelius (1914)	(+ ive)	Gravelius, 1914; Hidore, 1964; Avinash et al., 2011
Constant of Channel Maintenance (C_m)	$C_m = 1 / D_d$ where, D_d = Drainage density	Schumm (1956)	(+ ive)	Subba Rao, 2009; Avinash et al., 2011
Length of overland flow (L_o)	$L_o = 1 / 2D_d$ where, D_d = Drainage density	Horton (1945)	(+ ive)	Horton, 1945; Avinash et al., 2011
Basin Relief (B_r)	$B_r = H - h$, where, H = Maximum elevation in meter and h = Minimum elevation in meter	Hadley and Schumm (1961)	(–ive)	Hadley and Schumm, 1961; Subba Rao, 2009
Relief Ratio (R_r)	$R_r = R / L$; where, R = Basin relief; L = Longest axis in kilometre	Schumm (1956)	(–ive)	Srinivasa et al., 2008; Subba Rao, 2009
Ruggedness Index (RI)	$RI = B_r \times D_d$ where, RI = Ruggedness Index; B_r = Basin relief; D_d = Drainage density	Schumm (1956)	(–ive)	Biswas et al., 1999; Subba Rao, 2009
Mean Slope (S)	ASTER data based	Arc GIS v.9.3	(–ive)	Biswas et al., 1999; Avinash et al., 2011
Stream Gradient Ratio (S_g)	$S_g = (a - b)/ L$ where S_g = Stream Gradient ratio a = Elevation at source b = Elevation at mouth L = Longest axis in kilometre	Sreedevi et al., (2005)	(–ive)	Suja Rose and Krishnan, 2009
Travel Time (T_t)	$Tt = KL/ \sqrt{S}$, where, K = a proportional constant, L = Length of Main Stream, S = Slope of the Stream between two points	Kirpich (1940)	(+ ive)	Chow, 1964; Raghunath, 2013

ment of agricultural sector in the United States (Chow, 1964). A weighted CN has been calculated to obtain the potential maximum soil retention (S) capacity with intersecting land cover types and hydrological soil groups (Gundalia and Dholakia, 2014).

The CN values of different lands within the each sub-basin and grid have been derived from the reference table of CN calculations followed by Chow (1964). For this, basin-wise and grid-level land cover types have been extracted from direct observations using recent Google Earth images after superimposing the basin boundaries and grids over the image through Q-GIS. Once the curve numbers were identified for different land units, the weighted curve numbers were calculated for each basin and grid using Eq. (1).

$$\mathrm{WCN} = \frac{\sum (CN_1 \times a_1 + CN_2 \times a_2 + CN_n \times a_n)}{\sum a}, \quad (1)$$

where WCN is the weighted curve number, CN_1 is the curve number for particular land unit 1, a_1 is the area for that particular land unit 1, $\sum a$ is the sum of the total area. Next the derived WCN has been used to calculate the value of S, using Eq. (2). Eq. (3) has been used here to calculate the direct runoff from these basins and grids:

$$S = \frac{25400}{\mathrm{WCN}} - 254, \quad (2)$$

$$Q = \frac{(P - 0.2S)^2}{P + 0.8S}, \quad (3)$$

where Q denotes estimated direct runoff (mm), and P is maximum storm rainfall within a day (mm).

4.4 Integrated approach with geosciences and applied remote sensing

An integrated approach has been followed in the groundwater recharge potential mapping of the KRB. Geomorphology (drainage density, slope, ruggedness index), morphotectonics (lineament), geophysical parameters (Bouguer gravity anomaly), applied remote sensing, hydrological models (SCS Curve Number), and digital topography using topographic maps (1: 50,000), ASTER DEM (30 m), multi-spectral imageries (Landsat 8) and field mapping were all used. The approach deals with six most promising and widely used indices to delineate the zones of optimal groundwater recharge (Table 3).

The geomorphological features related to morphometric indices and all streams have been digitized from topographical maps at 1: 50,000 scale produced by the Survey of India (SoI) between 1967 and 1972. In addition, the online mapping system using 'Plug-in layer tool in Q-GIS software' with 'Google Satellite Image' was a useful technique for the extraction of features related to relief and linear geomorphology. ASTER DEM was used to prepare the slope map (in degrees) and the ruggedness index of the

Table 3 Techniques of different morphometric indices and their relationship with groundwater development

Morphometric indices	Source	Role on groundwater development (references)	Weightage values (W_v)
Drainage density (DD)/km^2	Topographical Maps, 1967 – 72 (1: 50,000)	(–ive) (Todd and Mays, 2005)	< 0 = 4 0 – 0.130 = 3 0.131 – 0.990 = 2 > 0.990 = 1
Surface slope (SS)/(°)	ASTER Dem, 2009 (30 m)	(–ive) (Biswas et al., 1999; Avinash et al., 2011)	< 1.7 = 4 1.71 – 3.397 = 3 3.398 – 5.430 = 2 > 5.430 = 1
Ruggedness index (RI)/km^2	ASTER Dem, 2009 (30 m)	(–ive) (Biswas et al., 1999; Subba Rao, 2009)	< 4.580 = 4 4.581 – 6.930 = 3 6.931 – 9.510 = 2 > 9.510 = 1
Lineament density (LD)/km^2	(NRSC, 2014)	(+ ive) (Yeh et al., 2014)	< 0.000075 = 1 0.000076 – 0.0840 = 2 0.0841 – 0.200 = 3 > 0.200 = 4
Bouguer gravity anomaly (BGA)/mGal	(NGRI, 1978)	(–ive) (Long and Kaufmann, 2013)	< 0 = 4 0 – 5 = 3 5 – 10 = 2 > 10 = 1
Maximum Water Retention Capacity (S)/mm	SCS Curve Number Method, (Chow, 1964; United States Department of Agriculture et al., 1999	(+ ive) (Chow, 1964)	< 55.76 = 1 55.76 – 63.50 = 2 63.51 – 108.85 = 3 > 108.85 = 4

KRB using Q-GIS. A web-based mapping technique was applied through the 'Layer from WM(T)S server' mapping tools in Q-GIS to get the arrangement of lineaments from the recently uploaded web version (http://bhuvan5.nrsc.gov.in/bhuvan/wms) in the thematic map services of the National Remote Sensing Centre (NRSC), India. According to NRSC (2014), it is a collaborative work of GIS cell of ISRO and the Standing Committee on Geology to prepare a national level geomorphological and lineament map on 1: 50,000 scale using a three-level classification system based on the origin of landforms. To prepare the density maps of digitized streamlines and lineaments, Kernel Function in Arc GIS v.9.3 has been run with the cell size of 30 m×30 m. We have also integrated the Bouguer gravity data to emphasize underlying rock density and its impact on the groundwater recharge. The map of Bouguer gravity anomalies was provided by the National Geophysical Research Institute or NGRI (1978), Hyderabad, India, with 5 mGal contour intervals, which has been converted into raster data using Q-GIS to extract the data in our study. Gridwise potential maximum retention of rainwater has also been calculated using the SCS Curve Number Method.

The above-mentioned factors were weighted and used to calculate a recharge potential score for the groundwater recharge zone. To consolidate all the data into a single framework and also to eliminate errors from the sub-basin wise generalizations, the KRB was divided into a set of grids (2,500 m per side). A total of 176 grids and their points were arranged over the study area and were used to extract the data from all six input maps. Map-wise data were classified into four groups based on their quartile ($Q_{1,\ 2,\ 3}$) values, thereafter, a weighted score (W_s) was assigned to each group within the range of 1–4 based on the relation with groundwater recharge. 'W_s 1' represents a very low potential zone for groundwater recharge and 'W_s 4' indicates optimum potentiality of water infiltration, whereas, W_s 2 and W_s 3 represent low and medium potential zones respectively (Table 3).

The cumulative weighted score for each grid (1 – 176) is computed using a weighted linear combination method by Eq. (4).

$$P_{r(1-176)} = DD_{wr} + SS_{wr} + RI_{wr} + LD_{wr} + BGA_{wr} + S_{wr}, \quad (4)$$

where $P_{r\ (1-176)}$ is the groundwater recharge potential index or cumulative weighted score of respective grids or points; *DD*, *SS*, *RI*, *LD*, *BGA*, and *S* are the score of drainage density (km/km^2), surface slope (°), ruggedness index (RI/km^2), lineament density (km/km^2), Bouguer gravity anomaly (mGal), and potential maximum water retention capacity (mm), respectively. The subscripts *w* and *r* refer to the weight of a theme and the reference number of individual points of the same theme, respectively. The generated vector file with points of cumulative weighted data has been interpolated using the inverse distance weighted (IDW) method (Philip and Watson, 1982) at the second power, with a variable search radius and considering the 12 closest points to prepare the final version of groundwater recharge potential map of the KRB. The potential groundwater recharge map in the basin has been divided into five grades, namely − excellent, good, moderate, low, and poor.

4.5 Model calibration by relative mean error calculation (RMEC)

To assess the efficiency of the results derived from the applied models for groundwater recharge monitoring, RMEC has been used to quantify the proximity and parallel conformity between observed and simulated rankings of sub-basins (Eq. (5)). The result, which has been derived from the seasonal water table fluctuation, is used as the reference/observed ranking in the comparison.

$$\mathrm{RME} = \frac{(BR_{ob} - BR_{ca}) \times 100}{BR_{ob}}, \quad (5)$$

where BR_{ob} is the sub-basin wise observed rank based on the seasonal water table fluctuation and BR_{ca} denotes the simulated rank of each basin based on their rank in three different techniques for groundwater recharge capability.

5 Results and analysis

5.1 Potentiality of groundwater recharge using basin morphometry

An individual, morphometric parameter based, sub-basin wise ranking method has been followed in respect to the role of these parameters on groundwater recharge (Tables 4 and 5). In ranking style, the 1st priority shows the most potential of groundwater storage while the last priority, i.e., 9th shows most impermeable area for groundwater recharge. With the sum of all ranks of each sub-basin for each parameter, a compound rank has been calculated, where a low value denotes the first priority and a high value indicates the least priority for groundwater recharge capability (Table 5).

Table 5 shows that the sub-basins I, D, and C, hold the first three ranks (1, 2, and 3) out of the nine sub-basins. Hydro-morphologically, these three sub basins are the most suitable for groundwater recharge. They share the characteristics of low stream frequency, drainage density, and drainage texture and high content of channel maintenance and high length of overland flow. Additionally, low basin relief low relative relief, low ruggedness index, low slope; and low stream gradient help to generate potential recharge zones within the KRB. Spatially, about 33.37% area of the total KRB has been identified as the most suitable zone for groundwater recharge. Hydro-

Table 4 Sub-basin wise extracted values of eighteen morphometric parameters of KRB

SB	Area/km^2	S_f	D_d	D_t	S_{tr}	B_R	F_F	E_R	C_R	S_F	C_C	C_M	L_O	B_r	R_r	R_I	S	S_g	T_t
A	58.75	0.80	1.13	0.90	1.63	1.94	0.3338	0.6517	0.641	3.00	1.25	0.88	0.44	34.66	2.77	39.17	0.248	1.97	01.8654
B	74.77	0.41	0.66	0.27	1.31	1.78	0.3230	0.6411	0.65	3.09	1.24	1.52	0.76	40.00	2.75	26.40	0.322	2.38	01.7024
C	58.10	0.15	0.38	0.06	1.33	4.00	0.3343	0.6522	0.68	2.99	1.21	2.63	1.32	17.31	1.45	6.58	0.126	0.17	02.2343
D	87.11	0.20	0.42	0.08	0.4	2.33	0.3164	0.6345	0.6	3.16	1.29	2.38	1.19	22.0	1.48	9.24	0.086	0.45	02.8164
E	113.28	0.38	0.42	0.16	1.71	2.39	0.3053	0.6232	0.61	3.27	1.28	2.38	1.19	32.05	1.72	13.46	0.167	1.55	01.6010
F	92.87	0.54	0.71	0.38	1.29	2.18	0.3136	0.6317	0.59	3.19	1.31	1.40	0.70	23.45	1.46	16.65	0.171	1.43	01.6214
G	191.27	0.22	0.69	0.15	0.71	1.97	0.2843	0.6014	0.64	3.52	1.26	1.45	0.72	39.87	1.99	27.51	0.15	0.11	28.0901
H	79.15	0.23	0.47	0.11	2.26	2.50	0.3205	0.6386	0.63	3.12	1.27	2.13	1.06	27.99	1.88	13.16	0.072	0.47	03.4776
I	160.31	0.26	0.54	0.14	1.48	2.02	0.2912	0.6087	0.57	3.43	1.33	1.85	0.93	14.42	0.75	7.79	0.078	0.17	09.6179

Table 5 Sub-basin wise groundwater recharge potential ranking based on morphometric parameters of the KRB

SB	S_f	D_d	D_t	S_{tr}	B_R	F_F	E_R	C_R	S_F	C_C	C_M	L_O	B_r	R_r	R_I	S	S_g	T_t	Total score	Rank
A	9	9	9	7	2	9	2	7	8	7	9	9	7	9	9	8	8	6	134	9
B	7	6	7	4	1	7	3	8	7	8	6	6	9	8	7	9	9	7	119	8
C	1	1	1	5	9	8	1	9	9	9	1	1	2	2	1	4	2	5	71	3
D	2	3	2	1	6	5	5	3	5	3	3	3	3	4	3	3	4	4	62	2
E	6	2	6	8	7	3	7	4	3	4	2	2	6	5	5	6	7	9	92	6
F	8	8	8	3	5	4	6	2	4	2	8	8	4	3	6	7	6	8	100	7
G	3	7	5	2	3	1	9	6	1	6	7	7	8	7	8	5	1	1	87	5
H	4	4	3	9	8	6	4	5	6	5	4	4	5	6	4	1	5	3	86	4
I	5	5	4	6	4	2	8	1	2	1	5	5	1	1	2	2	3	2	59	1

morphologically, results for A, B, and F are due to the inverse conditions in comparison with the sub-basins I, D, and C. These sub basins are the least suitable areas for groundwater recharge. Spatially, about 24.73% area of the total KRB comes under this heading. The rest of the basin is considered as a moderate zone for groundwater development.

5.2 Potentiality of groundwater recharge using SCS curve number method

Greater contact time between rainfall and the ground surface increases the rate of infiltration and amount of groundwater (Raghunath, 2013; Ahmad et al., 2015); these processes are also positively correlated with maximum water retention capacity (Chow, 1964; Shi et al., 2009; Raghunath, 2013). The result derived from the SCS curve number method shows the typical variation in water retention capacity and the amount of direct runoff due to the variation of land use/land cover characteristics over the sub-basins (Table 6). Sub-basin D has the maximum retention capacity (107.41 mm) with low (78.02 mm) direct runoff capacity. The current result shows that Sub-basin D has favorable conditions for groundwater recharge. Alternatively, in Sub-basin A, the largest percentage of rainwater (67.19%) is transferred into direct runoff (107.50 mm) and so the sub-basin experiences very low (56.86 mm) water retention capacity. It indicates the existence of a confined soil layer and lack of infiltration capacity.

5.3 Potentiality of groundwater recharge from integrated geosciences

5.3.1 Drainage density and groundwater recharge

In the KRB, drainage density (DD) ranges from 0.08 km/km^2 to 1.17 km/km^2, with an average density of 0.48 km/km^2 (Fig. 2(a)). The overall value illustrates the permeable nature of the basin surface strata: a coarse-drainage density (Ramalingam and Santhakumar, 2001). The lower drainage density at the edges of the basin helps rainwater to percolate or infiltrate towards the interior of the basin, a natural hydraulic gradient (Roy and Mistri, 2013).

5.3.2 Ruggedness index and groundwater recharge

Ruggedness Index (*RI*) is a combined result of basin relief (R) and drainage density (D_d) that indicates the structural complexity of the terrain (Schumm, 1956). A higher value

Table 6 Potential maximum retention and direct runoff characteristics of nine Sub-basin of the KRB during a strom event (19th September, 2000) using SCS curve number method

Sub-basin	Area/km^2	Hydrological soil types (with area in % of total and land use type)	Weighted CN value	*S*/mm	*P**/mm	*Q*/mm	% of total rainfall
A	58.75	B (61.34/Pa),C (38.66/Pa)	81.71	56.86	160	107.50	67.19
B	74.77	A (30.23/I),B (13.67/Pa),C (56.10/Pa)	76.80	76.73	160	94.52	59.08
C	58.10	C (89.31/TF),D (10.69/A)	77.43	74.04	160	96.16	60.10
D	87.11	B (3.18/Pa),C (96.82/DF)	70.28	107.41	160	78.02	48.76
E	113.28	C (73.05/DF),D (26.95/A)	75.66	81.71	160	91.57	57.23
F	92.89	C (98.23/DF),D (1.77/A)	70.37	106.95	160	78.24	48.90
G	191.27	C (53.35/A),D (46.65/A)	89.40	30.12	160	128.78	80.49
H	79.15	C (14.80/A),D (85.20/A)	90.56	26.48	160	132.09	82.56
I	160.31	D (100/A)	91.00	25.12	160	133.36	83.35

*Maximum one day rainfall on the 19th September, 2000 (River Research Institute, Kolkata); Station: Illambazar
Pa-pasture land, I-Industrial Area with 72% impervious land, TF-thin forest cover, DF-dense forest cover, A-agricultural land.

of *RI* indicates a zone of high topographic relief with steep, sloping ground and high drainage density (Ramalingam and Santhakumar, 2001; Avinash et al., 2014; Saravanan and Manjula, 2015). The inverse relationship of e *RI* with groundwater development suggests that a lower value of *RI* is favorable for rainwater infiltration. Over the KRB, *RI* values range from 2.55/km^2 to 16.07/km^2 with an average of 7.03/km^2 (Fig. 2(b)). Maximum *RI* values were calculated for the extreme northwestern and southeastern parts of the basin. Part of the middle basin had a medium to high *RI* value. Lower drainage density is typically associated with less rugged terrain.

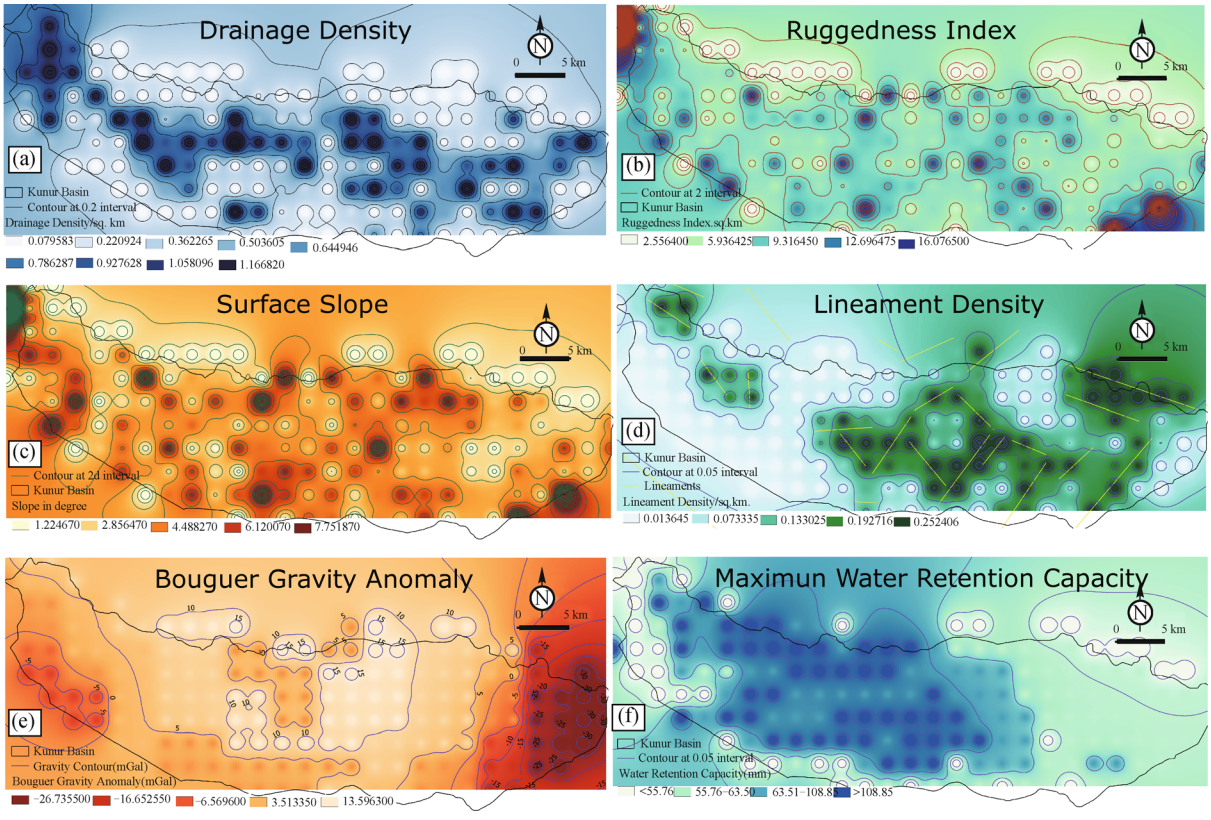

Fig. 2 (a–f): Applied indices from different field of geosciences to identify the groundwater recharge potential area over the Kunur River Basin.

5.3.3 Surface slope and groundwater recharge

Surface slope is the key indicator of all geomorphological studies and is controlled by climato-morphogenic processes working on areas with underlying rocks of varying resistance (Ramalingam and Santhakumar, 2001; Saravanan and Manjula, 2015). The understanding of slope properties is essential to identifying the spatial variation of surface runoff capacity and its travel time (Sreedevi et al., 2005). Flat and gently sloping ground promotes the maximum capacity of water infiltration and groundwater development, whereas a steeply sloping ground encourages speedy runoff and no infiltration (Subba Rao et al., 2001). In the present study area, the slope ranges from 1.22° to 7.75°, with an average 3.90° (Fig. 2(c)). A maximum portion of the land is identified as gently sloping ground and suggests good capacity for water infiltration. The basin has also steeply sloping land over the far upstream areas with additional small areas throughout the basin. The steeplysloping ground promotes immediate runoff of rainwater instead of infiltration (Subba Rao, 2009).

5.3.4 Lineaments and groundwater recharge

Lineaments provide easy pathways for groundwater movement and enhance groundwater recharge potential (Haridas et al., 1994, 1998; Sankar, 2002). The lineament density map is a measure of the quantitative length of linear features expressed in a grid. The lineament density of an area can indirectly reveal the groundwater potentiality of that area since the presence of lineaments usually denotes a permeable zone (Gopinath and Seralathan, 2004). In the KRB, a total of 20 lineaments have been traced which vary from 2.33 km to 15.33 km in length, with an average of 6.75 km (Fig. 2(d)). There are two major trends for lineaments in the basin – SW to NE and NW to SE. There is major concentration of lineaments in the middle of the Kunur basin along with the upper catchment area. The zones of lineament intersection have high capability of groundwater recharge (Gopinath and Seralathan, 2004), but there is no such intersection point in the KRB. In the lineament density map (Fig. 2(d)) value ranges from 0.013 km/km^2 to 0.250 km/km^2, where the average density is 0.114 km/km^2. Higher density areas have been observed over the middle part of the basin, the northeastern part of the downstream area, and the northwestern part of the upstream region.

5.3.5 Bouguer gravity anomaly and groundwater recharge

Understanding the underlying rock density is important for mapping the groundwater recharge area (Smith et al., 2004). According to Reddy (2005), the rate of infiltration is controlled by the fundamental properties of geological materials, mainly their density. However, the rate of infiltration is also controlled by the combined influence of gravity and capillary forces: gravity helps to move the excess water by deep percolation and builds up the groundwater table (Raghunath, 2013). Rock density plays an inverse relationship with the permeability of rock, and a positive relation with the porosity of rock (Reddy, 2005). Nevertheless, the permeability of rock positively controls the groundwater recharge capacity. The spatial variation of rock density beneath the surface has been widely estimated by gravity data (Prasad et al., 2005). According to Smith et al. (2004), gravity has the potential to be a new source of important remote sensing data for catchment-scale hydrological modeling. However, the usefulness of this data has not yet been demonstrated properly. Among the obtained gravity data from geophysical estimations, the Bouguer gravity data is more accurate and aids in standard geological interpretation of the land (USGS, 1997). According to Verma (1985), in an area underlain by rock with relatively high density, the Bouguer anomaly reflects a higher gravity and vice-versa. Bouguer anomalies are negative over elevated regions and show an inverse relationship with topography (USGS, 1997). The most important unknown source of the gravitational anomaly is the effect of the irregular underground distribution of different density rocks (USGS, 1997). According to Long and Kaufmann (2013), if the gravity anomaly is well defined, the excess or missing mass can be computed directly from the gravity data.

In the current study, the Bouguer gravity anomaly varies from -35 mGal to $+15$ mGal over the KRB (Fig. 2(e)). The minimum gravity value (-35 mGal) is observed over the extreme eastern part of the basin with a concentrated elliptical depression near the confluence zone with the Ajay River. Therefore, the bedrock of the downstream area may consist of young to old alluvium because of their lower density (1.50 – 2.0 g/cm^3) (Dobrin, 1976). Isolines of Bouguer gravity in the downstream area show a very rapid decrease of underlying rock density; within ten kilometres, gravity decreases from $+10$ mGal to -30 mGal. The high negative gravity values indicate the presence of low-density rock below the Ajay and Kunur Interfluve (AKI) region (Roy and Sahu, 2015). This gravitational depression might be the result of underlying sandy or unconsolidated sediment with a high percentage of granular material (Sahu and Saha, 2014).

Underlying heavy dense rock has been perceived in the middle of the basin from the maximum gravity anomaly. The lithological condition of this tract has been revealed by the panel diagram based on 12 exploratory boreholes (Fig. 3). The depth of the bedrock increases rapidly towards the downstream direction of the Kunur River (Roy and Sahu, 2015). The panel diagram over the palaeo-hydrological zone of the AKI region shows a large

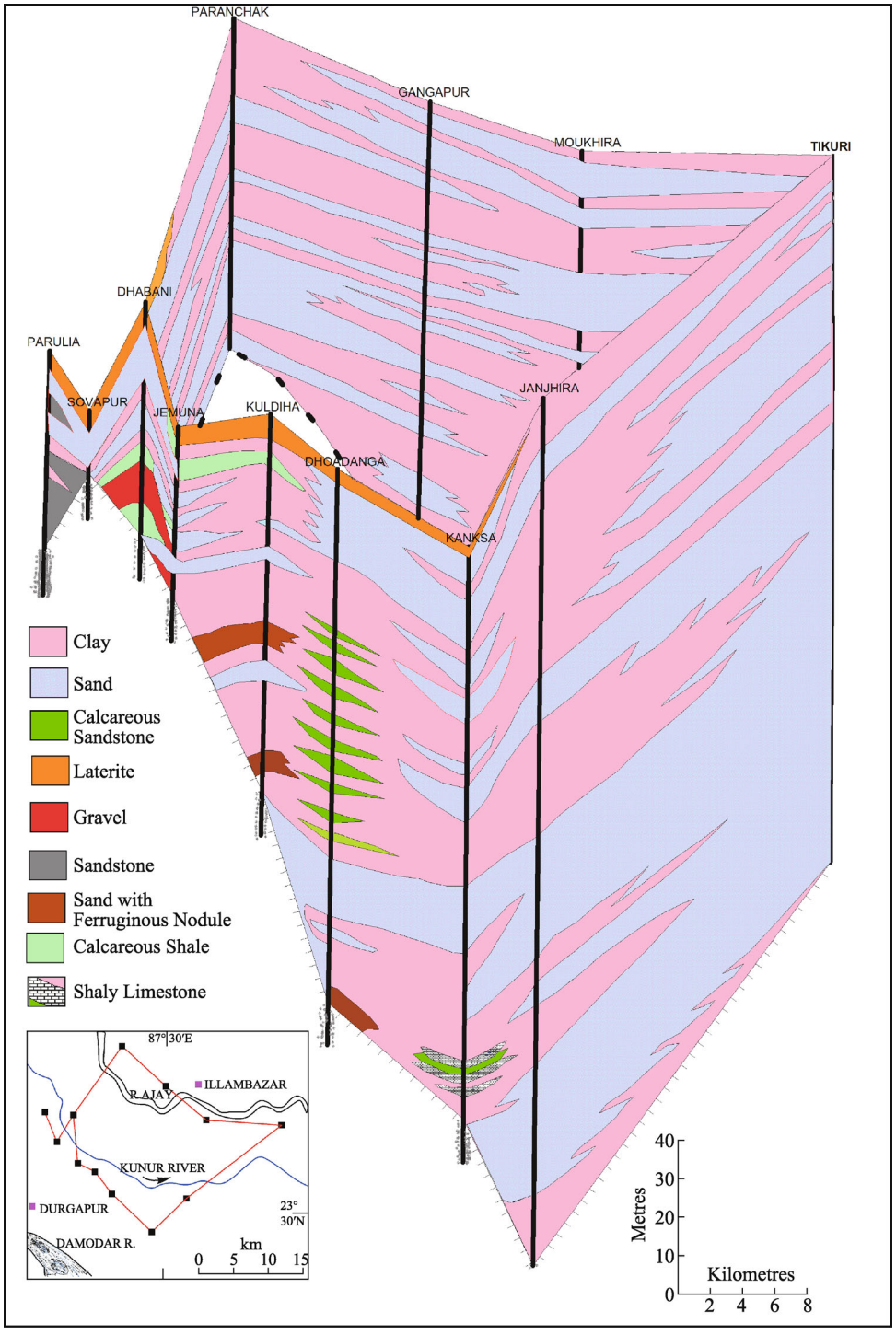

Fig. 3 Panel diagram showing the lithological condition in the Interfluve region of Ajay and Kunur rivers (Source: modified of Niyogi, 1985)

proportion of lithofacies consisting of sand and alternating thin layers of clay. 'Tikuri' (87.78581°E/23.54674°N) is an important borehole point in this zone for its location in the palaeochannels in the interfluve of the Ajay and Kunur Rivers; 86.50% of the 185 m of drilling at Tikuri consists of sandy material (Niyogi, 1985).

5.3.6 SCS curve number method and groundwater recharge

The SCS curve number method explores the close relationship between the land cover characteristics and the water infiltration capacity of different hydrological soil groups of the KRB. Maximum soil retention capacity

(> 108.85 mm) has been identified over the forest-dominated areas and the lowest retention capacity (< 55.76 mm) has observed over the *murrum* quarrying areas and expanding urban area of Durgapur Municipal Corporation (DMC) in the upper catchment (Fig. 2(f)). Recent satellite images are showing that 31.35% of the basin area is covered by dense *sal (shorea robusta)* forest and around 42% is under the agricultural land. *Sal* forests have great influence on altering hydrological behaviors of any area and induce high water retention capacity and less runoff (NIH, 1996 – 1997). The area with forest cover experiences higher water infiltration capacity than other land covers (Table 7). The dense *sal* forest cover in the middle of the basin increases the capacity of water infiltration and helps to intercept up to 25.30% of rainfall (NIH, 1996 – 1997).

Table 7 Role of land cover type on soil surface infiltration (after NIH, 1996 – 1997)

Land use	Infiltration rate/(cm·hr^{-1})
Forest	26.0
Grassland	12.0
Cropland	09.0
Grazed grassland	5.13
Cultivated land	7.20

5.3.7 Groundwater recharge potential zoning

The fusion derived map shows the regional variability of groundwater recharge potential over the KRB (Fig. 4). Four windows (W1–W4) have been selected for better understanding the causes of this scenario. Five potential groundwater recharge zones have been identified in the basin, where excellent zones for groundwater recharge have been found over the northeast part of the downstream area (W1) and in the northern part of upper catchment area (W2).

During the investigation of the background causes for the excellent recharge zones in the lower basin area, Landsat ETM+ images identified the presence of numerous palaeochannels in the band combination of 574 (Fig. 5(a)). This combination involves no visible light bands and provides the best atmospheric penetration capacity with better absorption rates in the water bodies. It may be used to find textural and moisture characteristics of soils. During a field survey near Guskara (87.73952°E; 23.49121°N), a suspected palaeochannel was identified over the floodplain area of the AKI region (Window 1; Fig. 5(a)-inset). Palaeochannels provide high infiltration capacity and work as a sub-surface pathway for groundwater movement in the sedimentary basin (Mallinson et al., 2010; Kolker et al., 2013). Therefore, this region of the KRB has a high groundwater recharge potential. Due to the significant role of palaeochannels on groundwater recharge, a comprehensive study of the palaeohydrology in India has begun from a series of works on palaeodischarge estimation (Sridhar, 2007; Sridhar et al., 2013), palaeochannel mapping (Zankhna and Thakkar, 2014), and reconstruction of palaeochannel morphology with palaeohydrological attributes (Khan and Tewari, 2011). Samadder et al. (2011) have mapped the locations of palaeochannels over the western Ganga plains to detect potential zones for groundwater research. Another excellent zone for groundwater recharge in the KRB is in the northern part of the upper basin area (Window 2; Fig. 5(b)) due to the presence of dense *sal* forest cover. A positive relationship

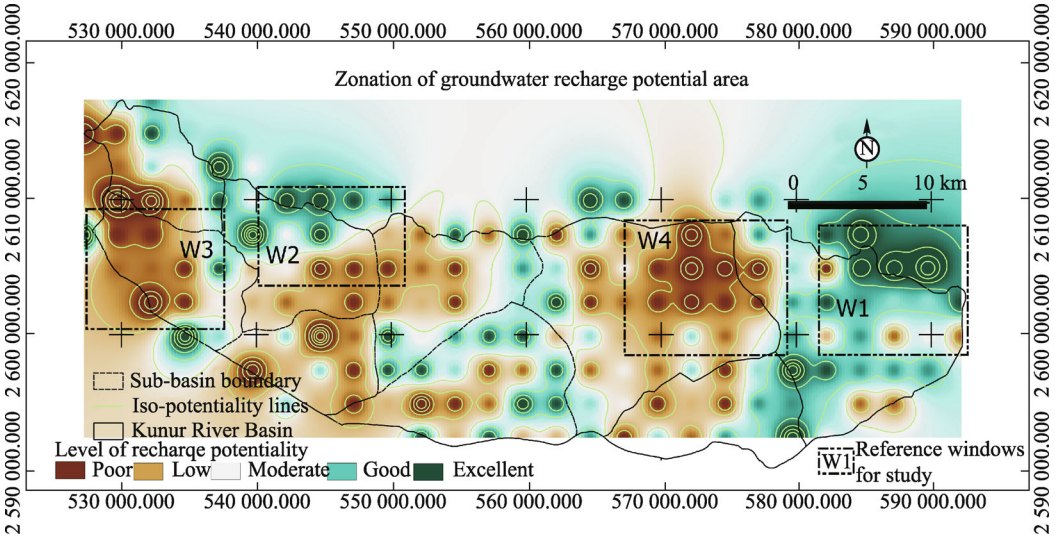

Fig. 4 Groundwater recharge potential map of the Kunur River Basin.

between forest cover and groundwater recharge capacity has been noticed in the basin. Some zones of moderate to good recharge capacity over middle of the basin area also exist due to the dense to open *sal* forest.

Due to human activities, a notable part of the basin area comes under the poor to low category of groundwater recharge zones. Two windows have been identified as the poorest areas for groundwater recharge (Window 3 and 4 in Fig. 4). Window 3 shows an extensive urban area of the Durgapur Municipal Corporation (DMC). Its increasingly paved land covers are the major cause for low infiltration capacity (Fig. 5(c)). In Window 4 (Fig. 5(d)), extensive agricultural practices have reduced the infiltration capacity (7.20 $cm \cdot hr^{-1}$) of the soil. The higher Bouguer gravity value also indicates that underlying dense rock plays an important role in developing poor to low categories of groundwater recharge zones (Fig. 2(e)).

Areas with good to excellent zones of recharge are also calculated for each sub-basin to prepare a ranking table (Table 8). Basin I holds first position with a maximum area (48.29%) under the good to excellent zone of recharge category. Basin H ranks second with 33.77%, followed by Basins D (25.06%), E (20.62%), A (16%), F (14.07%), B (5.51%), G (4.02%), and C (3.30%).

6 Discussion

Groundwater level data from twenty-four wells for the Pre-monsoon and Post-monsoon time periods of the last decade (2000 – 2010) have been used to calculate the average seasonal fluctuation of the water table over the KRB (Fig. 6). In order to generate a water table map, the data have been interpolated using the Kriging (NOTE: may be Kreiging, not Kriging) method. According to Saraf and Choudhury (1998), seasonal fluctuation of the water table is directly related to groundwater recharge. Subtraction of the Pre-monsoon water table from Post-monsoon water table image yields a water level fluctuation scenario. Maximum fluctuation (-3.5 m to -4.0 m) has been observed over the zones of W1 and W2 and in the middle of the basin, which are identified as excellent regions for groundwater recharge in Fig. 4. Contour lines of water table depth show that the Post-monsoon depth to the groundwater table (bgl) rose between 3.5 – 4.0 m from the Pre-monsoon level. Monsoon-fed rainfall is the major source of recharge in this region; the maximum infiltration capacity of rainwater in these zones recharges the ground-water table in the KRB. The minimal groundwater table fluctuation (< 2.0 m) has been observed over the identified

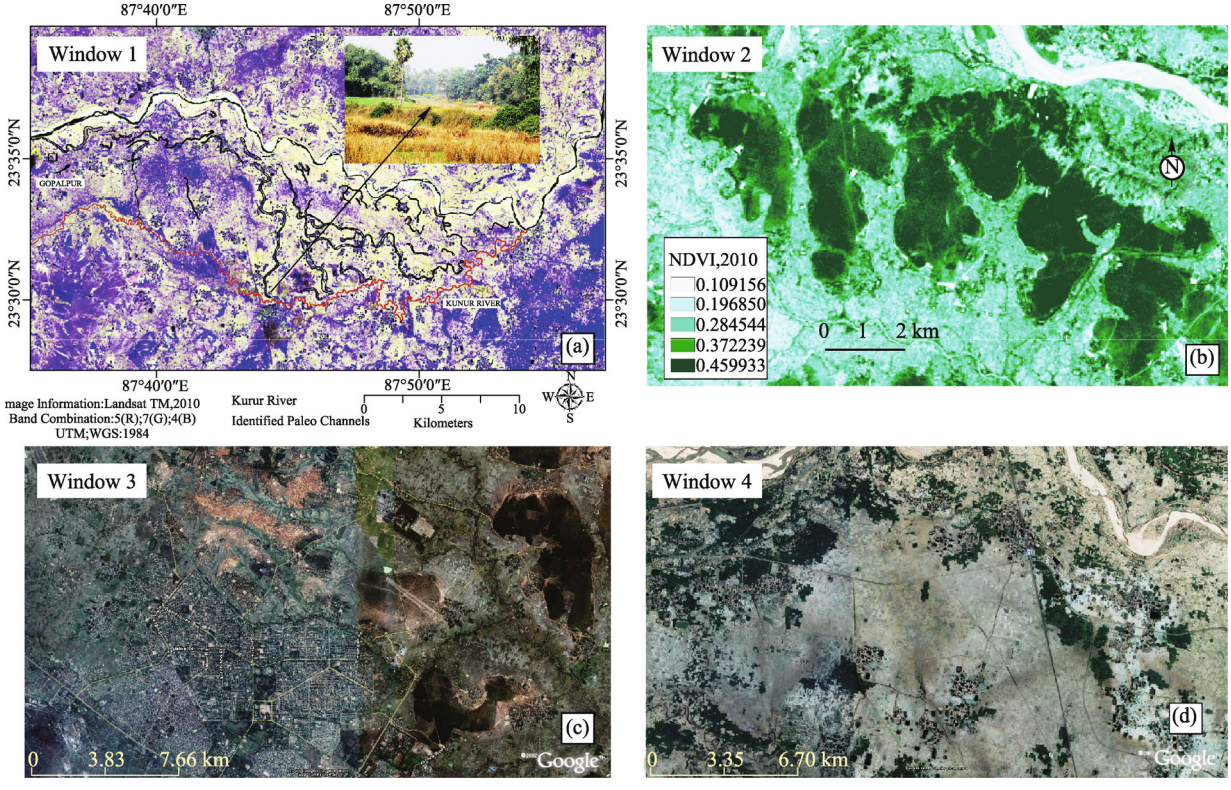

Fig. 5 Selected windows (W) for the case studies; (a) represents the highest potential zone for groundwater recharge due to the presence of numerous palaeochannels; (b) shows another excellent zone for groundwater recharge due to dense and healthy *sal (shorea robusta)* forest cover with higher NDVI values; (c) shows the extended urban area (DMC) acting as land impervious to recharge, and (d) is the zone of intensive agricultural cultivation and a poor zone for groundwater recharge.

poor zones for groundwater recharge, e.g., W3 and W4. The existence of extensive impervious land cover within W3 and the agricultural fields of W4 are the major causes for this situation. The visual relationship between Fig. 4 and Fig. 6 emphasizes this point on potential groundwater recharge zone identification.

In the present study, areas with groundwater fluctuation levels of more than 2.5 m bgl have been identified as suitable zones for groundwater recharge. Based on this, the areal coverage of good recharge capability zones have been calculated for each sub-basin separately and ranked (Table 8). This ranking order is the result of direct observation from the last ten years; therefore, this order has been taken as a standard level for calculating the relative mean error (RME) among the applied three techniques. Sub-basin I once again holds the first rank because the total area (100%) of this basin comes under the > 2.5 m bgl fluctuation level. Respectively, the remaining sub-basins are ranked from second, Sub-basin F, (90.61% covering area > 2.5m) through D (85.86%), H (68.73%), E (66.02%), G (51.63%), A (27.63%,), B (17.48%), and C (12.22%). The values from the RME calculation indicate that individual technique-based groundwater investigation is less effective than the multidisciplinary approach (Table 8). In order to most effectively conduct groundwater recharge potential mapping of the KRB, an integrated approach is more suitable than just using basin morphometry and the SCS curve number method. In this study, it has been also proved that the application of morphometric variables is more reliable than the simple remote sensing based hydrological model (SCS Curve Number). The efficiency of a geosciences base integrated study is also significant due to the higher correlation value (0.68 at 0.05% level of significance) between point wise observed groundwater table data and the cumulative recharge capability score from this technique.

7 Conclusions

The integrated field of geosciences confirms the better acceptability than basin morphometry and SCS curve number method for the potentiality mapping of groundwater recharge. Though, GRACE data has been proved as better alternative in recent days but this study proves surface geomorphological and geological characteristic and multispectral remote sensing data should be major ingredient in groundwater recharge area delineation for micro level study. This study also demonstrated that grid wise weighted index derived potentiality mapping is more feasible than sub-basin scale prioritization technique. The present study shows that the most effective groundwater recharge potential zones are locating downstream and within the forest belt of this basin. The role of forest cover on the development of groundwater table has also been proved. The negative impact of surface paving on the development of this valuable natural resource has been found over the DMC. The positive role of palaeochannels on groundwater recharge and development has been pointed out. Application of Bouguer gravity data and lineament density help to identify the effect of sub-surface conditions on the rate of water infiltration as well as

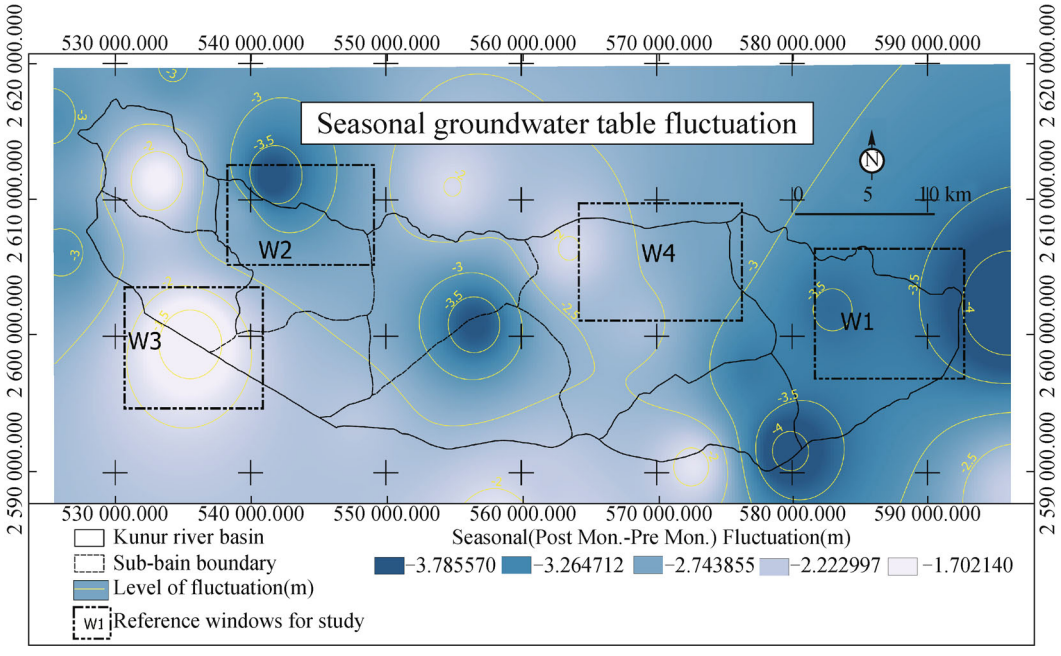

Fig. 6 Average seasonal fluctuation [post monsoon − pre monsoon] of the groundwater table over the KRB for the last decade (2000–2010), W1–W4 are showing the reference windows used in recharge potential map.

Table 8 Sub-basin wise ranking on the potentiality of groundwater recharge form different techniques to calculate the average relative mean error (RME)

Sub-basins	Ranks (based on the potentiality of groundwater recharge)			
	Basin morphometry wise	SCS CN method + applied remote sensing wise	Integrated geoscience wise	Seasonal recharge wise (observed data)
A	9	6	5	7
B	8	4	7	8
C	3	5	9	9
D	2	1	3	3
E	6	3	4	5
F	7	2	6	2
G	5	7	8	6
H	4	8	2	4
I	1	9	1	1
RME	46.14	125.78	38.26	Referenced rank

groundwater development. Overall, the study helps to distinguish those places which should be preserved as pathways for recharging groundwater for future utilization.

Acknowledgements Roy would like to thank and acknowledge University Grand Commission, New Delhi, India, for the financial support as Junior Research Fellowship [Award Letter No.:F.15-6(DEC.,2012)/2013(NET), UGC Ref. No. 3224/(NET-DEC.2012)] to carry out the research work presented in this paper. We also thank the anonymous reviewers and editors for their constructive comments.

References

Ahmad I, Verma V, Verma M K (2015). Application of Curve Number Method for Estimation of Runoff Potential in GIS Environment. 2nd International Conference on Geological and Civil Engineering, IPCBEE, 80, 16–20

Ajmal M, Moon G, Ahn J, Kim T (2015). Investigation of SCS-CN and its inspired modified models for runoff estimation in South Korean watersheds. J Hydro-environment Res, 9(4): 592–603

Anbazhagan S, Ramasamy S M, Das Gupta S (2005). Remote sensing and GIS for artificial recharge study, runoff estimation and planning in Ayyar basin, Tamil Nadu, India. Environ Geol, 48(2): 158–170

Avinash K, Deepika B, Jayappa K S (2014). Basin geomorphology and drainage morphometry parameters used as indicators for groundwater prospect: insight from geographical information system (GIS) technique. Journal of Earth Science, 25(6): 1018–1032

Avinash K, Jayappa K S, Deepika B (2011). Prioritization of sub-basins based on geomorphology and morphometric analysis using remote sensing and geographic information system (GIS) techniques. Geocarto Int, 26(7): 569–592

Banerjee T, Das A L, Mukhopadhyay S C (2011). Prioritisation of Silai sub watersheds for erosion management using drainage morphometry and soil erosion rates. Geogr Rev India, 73(4): 323–338

Biswas S, Sudhakar S, Desai V R (1999). Prioritization of sub-watersheds based on morphometric analysis of drainage basin: a remote sensing and GIS approach. Journal of the Indian Society of Remote Sensing, 27(3): 155–166

CGWB (Central Ground Water Board) (2010). Groundwater Scenario of India 2009–10. Ministry of Water Resources, Govt. of India

CGWB (Central Ground Water Board) (2014). Aquifer Systems of West Bengal. Ministry of Water Resources, Govt. of India, Eastern Region, Kolkata

Chaudhary B S, Kumar M, Roy A K, Ruhal D S (1996). Application of Remote sensing and Geographic Information Systems in Groundwater investigations in Sohna block, Gurgaon District, Haryana (India). In: International Archives of Photogrametry and Remote sensing Vienna, vol. XXXI, Part B6, 18–23

Chow V T (1964). Handbook of Applied Hydrology. New York: McGraw-Hill

de Alwis D A, Easton Z M, Dahlke H E, Philpot W D, Steenhuis T S (2007). Unsupervised classification of saturated areas using a time series of remotely sensed images. Hydrol Earth Syst Sci, 11(5): 1609–1620

Dobrin M B (1976). Introduction to Geophysical Prospecting. New York: McGraw-Hill Bock Company

Drury S A (1993). Image Interpretation in Geology. UK: Chapman & Hall

Elbeih S F (2015). An overview of integrated remote sensing and GIS for groundwater mapping in Egypt. Ain Shams Engineering Journal, 6 (1): 1–15

Elmahdy S I, Mohamed M M (2015). Automatic detection of near surface geological and hydrological features and investigating their influence on groundwater accumulation and salinity in southwest Egypt using remote sensing and GIS. Geocarto Int, 30(2): 132–144

Esper Angillieri M Y (2008). Morphometric analysis of Colanguil river basin and flash flood hazard, San Juan, Argentina. Environmental Geology, 55(1): 107–111

Falkenmark M (1994). Successfully coping with complex water scarcity: an issue of land/water integration. In: Gieske A, Gould J, eds. Proceedings of the Workshop on Integrated Water Resources Management, University of Botswana and Rural Industries Research Centre, Kanye-Gaborone, 11–26

Godebo T R (2005). Application of Remote Sensing and GIS for

Geological Investigation and Groundwater Potential Zone Identification, Southeastern Ethiopian Plateau, Bale Mountains and the Surrounding Areas. Thesis of M. Sc. Dissertation, Department of Earth Sciences, Addis Ababa University, 43

Gopinath G, Seralathan P (2004). Identification of Groundwater Prospective Zones Using IRS-ID LISS III and Pump Test Methods. Journal of Indian Society of Remote Sensing, 32(4): 329–342

Gravelius H (1914). Grundrifi der gesamten Gewcisserkunde. Band I: Flufikunde (Compendium of Hydrology, vol. I. Rivers, in German). Germany: Goschen, Berlin

Gundalia M, Dholakia M (2014). Impact of Monthly Curve Number on Daily Runoff Estimation for Ozat Catchment in India. Open Journal of Modern Hydrology, 4(04): 144–155

Guo K, Wang J, Wang Y (2015). Application of ZY-3 remote sensing image in the research of Huashan experimental watershed. Proceedings of the International Association of Hydrological Sciences, 368: 51–56

Hadley R F, Schumm S A (1961). Sediment sources and drainage basin characteristics in upper Cheyenne River basin. Washington, DC: US Geological Survey, Water-Supply Paper. 1531–B, 198

Hajam R A, Hamid A, Bhat S (2013). Application of morphometric analysis for geo-hydrological studies using geo-spatial technology- A case study of Vishav Drainage Basin. Hydrol Current Res, 4: 157

Haridas V R, Aravmdan S, Gopinath G (1998). Remote sensing and its applications for groundwater favourable area identification. Qut J GARC, 6(1): 18–22

Haridas V R, Chandra Sekaran V A, Kumaraswamy K, Rajendran S, Unnikrishnan K (1994). Geomorphological and lineament studies of Kanjamalai using IRS-IA data with special reference to groundwater potentiality. Trans Inst Indian Geogr, 16(1): 35–41

Hidore J J (1964). Landform characteristics affecting watershed yields on the Mississippi–Missouri interfluve. In: Moore G A, ed. Proceedings of the Oklahoma Academy of Science. Edmond, Oklahoma: University of Central Oklahoma, 201–203

Horton R E (1932). Drainage basin characteristics. Trans Am Geophys Union, 13(1): 350–361

Horton R E (1945). Erosional development of streams and their drainage basins: hydro physical approach to quantitative morphology. Geol Soc Am Bull, 56(3): 275–370

Indian Meteorological Department (2014). IMD District wise normals, Barddhaman. Govt. of India

Javed A, Khanday Y M, Ahmed R (2009). Prioritization of sub-watersheds based on morphometric and land use analysis using remote sensing and GIS techniques. Journal of Indian Society of Remote Sensing, 37(2): 261–274

Jiang D, Wang J, Huang Y, Zhou K, Ding X, Fu J (2014). The Review of GRACE Data Applications in Terrestrial Hydrology Monitoring. Advances in Meteorology, Volume 2014, Article ID 725131, 9 pages, http://dx.doi.org/10.1155/2014/725131

Kale V S, Gupta A (2001). Introduction to geomorphology. Hyderabad, India: Orient Longman Ltd

Khan M A, Gupta V P, Moharana P C (2001). Watershed prioritization using remote sensing and geographical information system: a case study from Guhiya. India. J Arid Environ, 49(3): 465–475

Khan Z A, Tewari R C (2011). Palaeochannel and palaeohydrology of a Middle Siwalik (Pliocene) fluvial system, northern India. J Earth Syst Sci, 120(3): 531–543

Kirpich Z P (1940). Time of concentration of small agricultural watersheds. Civ Eng (NYNY), 6: 362

Kolker A S, Cable J E, Johannesson K H, Allison M A, Inniss L V (2013). Pathways and processes associated with the transport of groundwater in deltaic systems. J Hydrol (Amst), 498: 319–334

Koopmans B N (1983). Side looking Radar, a tool for geological surveys. Remote Sens Rev, 1(1): 19–69

Krishnamurthy J, Venkatesa Kumar N, Jayaraman V, Manivel M (1996). An approach to demarcate groundwater potential zones through remote sensing and a geographical information system. Int J Remote Sens, 17(10): 1867–1884

Kumar R, Raj H (2013). Mitigation of groundwater depletion hazards in India. Curr Sci, 104(10): 1271

Long D, Scanlon B R, Longuevergne L, Sun A Y, Fernando D N, Save H (2013). GRACE satellite monitoring of large depletion in water storage in response to the 2011 drought in Texas. Geophys Res Lett, 40(13): 3395–3401

Long D, Shen Y, Sun A, Hong Y, Longuevergne L, Yang Y, Li B, Chen L (2014). Drought and flood monitoring for a large karst plateau in Southwest China using extended GRACE data. Remote Sens Environ, 155: 145–160

Long L T, Kaufmann R D (2013). Acquisition and Analysis of Terrestrial Gravity Data. Delhi: Cambridge University Press

Longuevergne L, Scanlon B R, Wilson C R (2010). GRACE Hydrological estimates for small basins: evaluating processing approaches on the High Plains Aquifer, USA. Water Resour Res, 46(11): W11517

Magesh N S, Jitheshal K V, Chandrasekar N, Jini K V (2013). Geographical information system based morphometric analysis of Bharathapuzha River Basin, Kerla, India. Appl Water Sci, 3(2): 467–477

Mallinson D J, Smith C W, Culver S J, Riggs S R, Ames D (2010). Geological characteristics and spatial distribution of paleo-inlet channels beneath the outer banks barrier islands, North Carolina, USA. Estuar Coast Shelf Sci, 88(2): 175–189

Manu M S, Anirudhan S (2008). Drainage characteristics of Achankovil river basin, Kerala. J Geol Soc India, 71: 841–850

Martin A K, Gadiga B L (2015). Hydrological and Morphometric Analysis of Upper Yedzaram Catchmnet of Mubi in Adamawa State, Nigeria Using Geographical Information System (GIS). World Environment, 5(2): 63–69

McCauley J, Schaber F, Breed C S, Grolier M J, Haynes C V, Issawa B, Elachi C, Blom R (1982). Subsurface valleys and geo-archeology of the eastern Sahara revealed by Shuttle radar. Science, 218(4576): 1004–1020

Meijerink A M G (1996). Remote sensing applications to hydrology: groundwater. Hydrol Sci J, 41(4): 549–561

Menenti M, LI X, Wang J, Vereecken H, LI J, Mnacini M, Liu Q, Jia L, Kuenzer C, Huang S, Yesou H, Wen J, Ker Y, Cheng X, Gourmelen N, KE C, Ludwing R, LIN H, Eineder M, MA Y, Su ZB (2015). Hydrologic and Cryospheric Processes Observed From Space. The International Archives of the Photogrammetry, Remote Sensing and Spatial Information Sciences, XL (7/W3): 1101–1110

Miller V C (1953). A quantitative geomorphic study of drainage basin characteristics in the Clinch mountain area. New York: Department of

Geology, ONR, Columbia University, Virginia and Tennessee, Project NR389–402, Technical Report 3

Minor Irrigation Census (2001). Report on Census of Minor Irrigation Schemes (1993 – 94). Minor Irrigation Division, Ministry of Water Resources, Govt. of India, New Delhi

National Climate Centre (2006). Trends in the rainfall pattern over the India. India Meteorological Department, Pune, India

NGRI (1978). NGRI/GPH-1 to 5: Gravity Maps of India scale 1: 5,000,000. National Geophysical Research Institute, Hyderabad, India

NIH (National Institute of Hydrology) (1996 – 1997). Infiltration Studies in Sher-Umar River Doab in Narmada basin. Report No. CS (AR) 6/ 96-97, Jal Vighyan Bhawan, Roorkee, India

Niyogi M (1985). Groundwater resource of the Ajay Basin. In: Chatterjee S P, ed. Geographical Mosaic- Professor K.G. Bagechi Felicitation, Manasi Press, Calcutta, India, 165–182

Nooka Ratnam K, Srivastava Y K, Venkateswara Rao V, Amminedu E, Murthy K S R (2005). Check dam positioning by prioritization of micro watersheds using SYI model and morphometric analysis – remote sensing and GIS perspective. Journal of the Indian Society of Remote Sensing, 33(1): 25–38

NRSC (2014). National geomorphological and lineament mapping on 1:50,000 scale using Resourcesat-1 LISS-III data. Manual for Geomorphology and Lineament Mapping (Web Version), National Remote Sensing Centre, Hyderabad, India

Obi Reddy G P, Maji A K, Gajbhiye K S (2004). Drainage morphometry and its influence on landform characteristics in a basaltic terrain, central India: a remote sensing and GIS approach. Int J Appl Earth Obs Geoinf, 6(1): 1–16

Pakhmode V, Kulkarni H, Deolankar S B (2003). Hydrological-drainage analysis in watershed-programme planning: a case from the Deccan basalt, India. Hydrogeol J, 11(5): 595–604

Philip G M, Watson D F (1982). A precise method for determining contoured surfaces. Aust Petrol Explor Assoc J, 22(1): 205–212

Prakash S R, Mishra D (1993). Identification of groundwater prospecting zones by using remote sensing and geoelectrical methods in and around Saidnager area, Dakar Block, Jalaun district, uttar pradesh. Indian Society of Remote Sensing, 21(4): 217–227

Prasad A S S S R S, Venkateswarlu N, Reddy P R (2005). Crustal density model along Gopali- Port Canning profile, West Bengal basin using seismic and gravity data. J Ind Geophys Union, 9(4): 235–239

Raghunath H M (2013). Hydrology: Principal, Analysis, Design (2nd Revised Ed.). New Delhi: New Age International Publishers

Rajwant, SharmaU K (2015). Morphometric analysis of third order river basins to assess the vulnerability of Baner Khad Watershed towards erosional process, Himachal Pradesh, India. Himalayan Geology, 36 (1): 65–73

Ramalingam M, Santhakumar A R (2001). Case study on artificial recharge using remote sensing and GIS. www.GISdevelopment.net, accessed on January 2, 2014

Ramamoorthi A (1983). Snow-melt run-off studies using remote sensing data. Sadhana, 6: 279–286

Rango A, Ritchie J C (1996). Remote sensing application to hydrology. Hydrol Sci J, 41(4): 477–494

Ravindran K V, Jeyram A (1997). Groundwater prospects of Shahbad tehsil, Baran district and eastern Rajasthan: a remote sensing approach. Indian society of remote sensing, 25 (4): 239–246

Reddy J R (2005). A Textbook of Hydrology. New Delhi: University Science Press

Ringrose S, Vanderpost C, Matheson W (1998). Evaluation of vegetative criteria for near-surface groundwater detection using multispectral mapping and GIS techniques in semi-arid Botswana. Appl Geogr, 18 (4): 331–354

Roy A K, Ray P K C (1993). Groundwater investigation using remote sensing and geographic information techniques- A case study in Manabazar-II, Purulia (W.B.). Proceeding national symposium of north-eastern region, Guwahati, India, 180–184

Roy S, Mistri B (2013). Estimation of peak flood discharge for an ungauged river: a case study of the Kunur River, West Bengal. Geogr J, 2013(214140): 1–11

Roy S, Sahu A S (2015). Quaternary tectonic control on channel morphology over sedimentary low land: a case study in the Ajay-Damodar interfluve of Eastern India. Geoscience Frontiers, 6(6): 927–946

Sahu S, Saha D (2014). Geomorphologic, stratigraphic and sedimentologic evidences of tectonic activity in Sone–Ganga alluvial tract in Middle Ganga Plain, India. J Earth Syst Sci, 123:1335–1347

Samadder R K, Kumar S, Gupta R P (2011). Palaeochannels and their potential for artificial groundwater recharge in the western Ganga plains. J Hydrol (Amst), 400(1 – 2): 154–164

Sankar K (2002). Evaluation of groundwater potential zones using remote sensing data in Upper Vaigai river basin, Tamil Nadu. India J Indian Soc Rem Sens, 30(3): 119–129

Saraf A K, Choudhury P R (1998). Integrated remote sensing and GIS for groundwater exploration and identification of artificial recharge sites. Int J Remote Sens, 19(10): 1825–1841

Saravanan S, Manjula R (2015). Geomorphology based semi-distributed approach for modeling rainfall-runoff modeling using GIS. Aquatic Procedia, 4: 908–916

Schultz G A (1997). Use of remote sensing data in a GIS environment for water resources management, Remote Sensing and Geographic Information Systems for Design and Operation of Water Resources Systems. In: Proceedings of Rabat Symposium S3, April 1997. IAHS Publ no. 242, 3–15

Schumm S A (1956). Evolution of drainage system and slope in badlands at Perth Amboy, New Jersey. Geol Soc Am Bull, 67(5): 597–646

Shah T (2009). Taming the Anarchy: Groundwater Governance in South Asia. Resources for the Future, Washington DC and International Water Management Institute, Colombo

Shah T (2011). Innovations in Groundwater Management: Examples from India. International Water Management Institute. http://rosenberg.ucanr.org/documents/argentina/Tushar ShahFinal.pdf

Shankar V P S, Kulkarni H, Krishnan S (2011). India's groundwater challenge and the way forward. Econ Polit Wkly, XLVI(2): 37–45

Shi J, Wang J, Hsu A Y, O'Neill P E, Engman E T (1997). Estimation of bare surface soil moisture and surface roughness parameter using L-band SAR image data. IEEE Trans Geosci Rem Sens, 35(5): 1254–1266

Shi Z H, Chen L D, Fang N F, Qin D F, Cai C F (2009). Research on the SCS CN initial abstraction ratio using rainfall-runoff event analysis in the Three Gorges Area, China. Catena, 77(1): 1–7

Smith A B, Walker J P, Western A W (2004). Assimilation of gravity data into a soil moisture and groundwater column model. In: Teuling A J, Leijnse H, Troch P A, Sheffield J, Wood E, F, eds. Proceedings of the 2nd international CAHMDA workshop on: The Terrestrial Water Cycle: Modelling and Data Assimilation Across Catchment Scales, Princeton, NJ, 135–137

Smith K G (1950). Standards for grading texture of erosional topography. American Journal of Science, 248: 655–668

Soil Conservation Service (1964). National engineering handbook. Section 4, Hydrology, Department of Agriculture, Washington, 450

Soil Conservation Service (1972). National engineering handbook. Section 4, Hydrology, Department of Agriculture, Washington, 762

Sreedevi P D, Subrahmanyam K, Ahmed S (2005). The significance of morphometric analysis for obtaining groundwater potential zones in a structurally controlled terrain. Environmental Geology, 47(3): 412–420

Sridhar A (2007). Discharge estimation from planform characters of the Shedhi River, Gujarat alluvial plain: present and past. J Earth Syst Sci, 116(4): 341–346

Sridhar A, Chamyal L S, Bhattacharjee F, Singhvi A K (2013). Early Holocene fluvial activity from the sedimentology and palaeohydrology of gravel terrace in the semi arid Mahi River Basin, India. J Asian Earth Sci, 66: 240–248

Srinivasa V S, Govindaiah S, Honne Gowda H (2008). Prioritization of sub-watersheds for sustainable development and management of natural resources: an integrated approach using remote sensing, GIS and socio-economic data. Curr Sci, 95: 345–354

Strahler A N (1957). Quantative Analysis of Watershed geomorphology. Transactions. American Geophysical Union, 38(6): 913–920

Strahler A N (1964). Quantitative geomorphology of drainage and channel networks. In: Chow V T, ed. Handbook of Applied Hydrology. New York: McGraw Hill Book Company, 439–476

Subba Rao N (2009). A numerical scheme for groundwater development in a watershed basin of basement terrain: a case study from India. Hydrogeol J, 17(2): 379–396

Subba Rao N, Chakradhar G K J, Srinivas V (2001). Identification of groundwater potential zones using remote sensing techniques in and around Guntur Town, Andhra Pradesh, India. Journal of Indian Society of Remote Sensing, 29(1&2): 69–78

Suja Rose R S, Krishnan N (2009). Spatial analysis of groundwater potential using remote sensing and GIS in the Kanyakumari and Nambiyar Basins, India. J Indian Soc Remote Sens, 37(4): 681–692

Suresh M, Sudhakar S, Tiwari K N, Chowdary V M (2004). Prioritization of watersheds using morphometric parameters and assessment of surface water potential using remote sensing. Journal of the Indian Society of Remote Sensing, 32(3): 249–259

Thakkar A K, Dhiman S D (2007). Morphometric analysis and prioritization of miniwatersheds in Mohr watershed, Gujarat, using remote sensing and GIS techniques. Journal of the Indian Society of Remote Sensing, 35(4): 313–321

Todd D K, Mays L W (2005). Groundwater Hydrology (3rd edition). New York: John Wiley & Sons, 636

United State Geological Society (1997). Introduction to Potential Fields: Gravity. FS-239-95. Available onhttp://pubs.usgs.gov/fs/fs-0239-95/fs-0239-95.pdf, retrieved on 13th December, 2014

United States Department of Agriculture, Natural Resource Conservation Service, and National Employee Development Centre (1999). SCS Runoff Equation: Module 205. Engineering and Hydrology Training Series, 1–27

van Dijk A I J M, Renzullo L J (2011). Water resource monitoring systems and the role of satellite observations. Hydrol Earth Syst Sci, 15(1): 39–55

Verma R K (1985). Gravity field, seismicity, and tectonics of the Indian peninsula and the Himalayas (Solid earth sciences library). Holland: D. Reidel Publishing Company

Wagener T, Wheater H S, Gupta H V (2004). Rainfall-Runoff Modelling In: Gauged and Ungauged Catchments. London: Imperial College Press

Wagner W, Naeimi V, Scipal K, de Jeu R, Martinez-Fernandez J (2007). Soil moisture from operational meteorological satellites. Journal of Hydrogeology, 15(1): 121–131

Wahr J, Swenson S, Zlotnicki V, Velicogna I (2004). Timevariable gravity from GRACE: fist results. Geophys Res Lett, 31(11): L11501

Yeh H F, Lin H I, Lee S T, Chang M H, Hsu K C, Lee C H (2014). GIS and SBF for estimating groundwater recharge of a mountainous basin in the Wu River watershed, Taiwan. J Earth Syst Sci, 123(3): 503–516

Zankhna S, Thakkar M G (2014). Palaeochannel investigations and geo hydrological significance of Saraswati River of Mainland Gujarat, India: using remote sensing and GIS techniques. J Environ Res Develop, 9(2): 472–479

Zhang H Y, Shi Z H, Fang N F, Guo M H (2015). Linking watershed geomorphic characteristics to sediment yield: evidence from the Loess Plateau of China. Geomorphology, 234: 19–27